Analysis and Design of Three-Coil Wireless Power Transfer System with Split Transmitting Coils

Zanfeng Fang
State Key Laboratory of AMS-VLSI,
Institute of Microelectronics, and
Faculty of Science and Technology
University of Macau, Macao, China
fred.fangzf@connect.um.edu.mo

Wenxing Zhong
College of Electrical Engineering
Zhejiang University
Hangzhou, China
wxzhong@zju.edu.cn

Yan Lu
State Key Laboratory of AMS-VLSI,
Institute of Microelectronics, and
Faculty of Science and Technology
University of Macau, Macao, China
yanlu@um.edu.mo

***Abstract*—Wireless power transfer (WPT) technology is helping the electric vehicles (EVs) to solve several issues brought by cable charging. Three different WPT networks, namely series-series (SS), three-coil, and inductor-capacitor-capacitor-series (LCC-S), are the possibilities for different application scenarios. This paper analyzes the three-coil WPT system and compares it with the other two networks. We find that the three-coil network is combining the advantages of the other two networks, including high efficiency and better misalignment tolerance. Then, we have concluded several conditions to guide the design of three-coil WPT system. Next, we propose a design method, that is setting the turn ratio to split the transmitter coil of an SS network into two independent coils and the compensation capacitors to meet the conditions above. Finally, we obtain experimental results with 3.3kW output and 96.67% total efficiency, using a split transmitting three-coil network.**

Keywords—wireless power transfer (WPT); three-coil; series-series (SS); inductor-capacitor-capacitor-series (LCC-S)

I. Introduction

Electric vehicles (EVs) are of great importance in helping to reduce the carbon emissions produced by gasoline-powered vehicles. Until now, most EVs are charged in a plug-in way. To promote the applications of EVs and smart grid, lots of charging stations were built, but their safety issues are still a concern. For example, people may be tripped over by the cable on the floor, and the harsh climate conditions or cracked old cable may bring an electric shock.

On the other hand, the wireless power transfer (WPT) technology provides a good alternative to eliminate all the safety troubles caused by plug-in charging. Charging without cables can provide not only stationary but also dynamic methods for safe charging [1]-[3].

Basically, for the better use of EV charging, the resonant frequency and compensation network should be well-designed. It is imperative that choosing a compensation network is of great help in improving the WPT system's efficiency and output power. In general, the compensated network could determine the upper limit of the output power of the WPT system, where the series-series (SS) and inductor-capacitor-capacitor-series (LCC-S) compensation networks are commonly used. An SS network can simply control the charging current to output constant-current [4], while an LCC-S network can realize a constant charging profile over a wide range of pad misalignment [5]. However, for an SS network, when the EV leaves the charging pad, which means the coupling coefficient reduces, the voltage gain will increase, and some protections need to be used to prevent the over-voltage [6]. For an LCC-S network, the additional inductor results in the increase of volume, weight and cost.

Then, the three-coil network was then proposed [7]. Even though the volume of a three-coil network can be the same as an SS network by placing its additional coil on the same plane as the transmitter or the receiver, a three-coil network still performs better on reducing the current stress and over-voltage caused by misalignment [8]. Nonetheless, a three-coil network need to be well-designed to achieve the advantages mentioned above. The work in [9] designed a three-coil WPT system with constant-voltage and constant-current charging by adding the additional coil individually, which did not make full use of the receiver coil space in the SS network. [10] improves the three-coil network efficiency by using an additional coil to extent the transfer distance with all free-resonant-frequency method, which may not be suitable for space-limited application.

This paper aims to analyze and design an optimized three-coil WPT system with split transmitting coils. This method sets the turn ratio to split the transmitter coil of an SS network into two independent coils and the compensation capacitors. Furthermore, the proposed method would make a full use of the transmitter and receiver area. The paper is organized as follows. Section II introduces the basics about WPT networks, and compares the three compensation networks including the SS, three-coil, and LCC-S. Section III performs theoretical analyses with circuit modeling and simulations. The designs of the three-coil WPT system are then proposed in Section IV. Section V shows simulation and experimental results validating the analyses. Finally, Section VI draws concluding remarks.

II. Basic Power Transfer Network

A general WPT topology is shown in Fig. 1(a), including a source, a power transfer network (PTN), and a load. Usually, a source is formed by a full-bridge inverter with the DC voltage input to provide enough energy, where the fundamental phasor root mean square (RMS) of the inverter output is defined as

$$\mathbf{U_i} = \left(2\sqrt{2} \cdot U_{idc} / \pi\right) \cdot \sin\delta/2 \angle 0^{\circ} \tag{1}$$

2024 IEEE 7th International Electrical and Energy Conference (CIEEC) | 979-8-3503-5955-8/24/$31.00 ©2024 IEEE | DOI: 10.1109/CIEEC60922.2024.10583502

979-8-3503-5955-8/24/$31.00 ©2024 IEEE

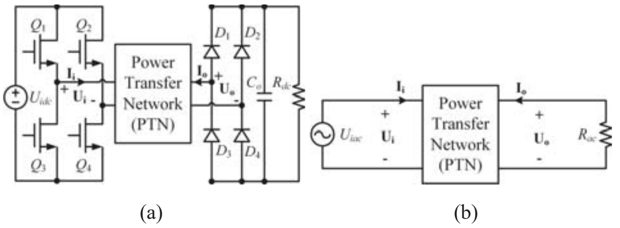

Fig. 1. A general WPT topology. (a) WPT system. (b) Ideal model.

where $\mathbf{U_i}$ is the input voltage phasor while U_{idc} is the input DC voltage, and δ is its conduction angle. Besides, an equivalent load (R_{ac}) can be expressed with the rectifier and the pure resistance DC load (R_{dc}) by

$$R_{ac} = 8 \cdot R_{dc} / \pi^2 \tag{2}$$

Hence, the equivalent RMS value of the rectifier input voltage $\mathbf{U_o}$ can be given as

$$\mathbf{U_o} = 2\sqrt{2} \cdot U_{dc} / \pi \tag{3}$$

where U_{dc} is the voltage of the DC load.

An ideal WPT circuit model is used as shown in Fig. 1(b), in which $\mathbf{I_i}$ and $\mathbf{I_o}$ are the input and output current phasor, respectively. Based on this model, the characteristics of the WPT system, such as the voltage gain, output power, power transfer efficiency and input impedance, can be easily calculated.

PTN can be realized by different structures. Due to the simple structure and small volume, the SS network shown in Fig. 2(a) is widely used in most WPT applications. Based on this structure, separating the transmitter coil (L_{s1}) into two independent coils (L_{t1} and L_{t2}) can easily obtain the three-coil network shown in Fig. 2(c) while adding another compensation inductor and capacitor can obtain the LCC-S network shown in Fig. 2(b). Compared with the SS network, the three-coil network has two extra mutual inductances (M_{t12} and M_{t13}), which means it has more design freedom without changing the volume. Besides, compared with the LCC-S network, the control of the three-coil network is relatively simpler. These three networks are further compared in the next section based on the following compensation conditions.

For the SS network, the angular frequency is defined as

$$\omega_0 = 1 / \sqrt{L_{s1} C_{s1}} = 1 / \sqrt{L_{s2} C_{s2}} \tag{4}$$

where L_{s1} and L_{s2} are the self-inductances of the transmitter coil and receiver coil, respectively, C_{s1} and C_{s2} are the compensation capacitances of the transmitter coil and receiver coil, respectively.

For the LCC-S network, the angular frequency is defined as

$$\omega_0 = 1 / \sqrt{L_f C_f} = 1 / \sqrt{\left(L_1 - L_f\right) C_1} = 1 / \sqrt{L_2 C_2} \tag{5}$$

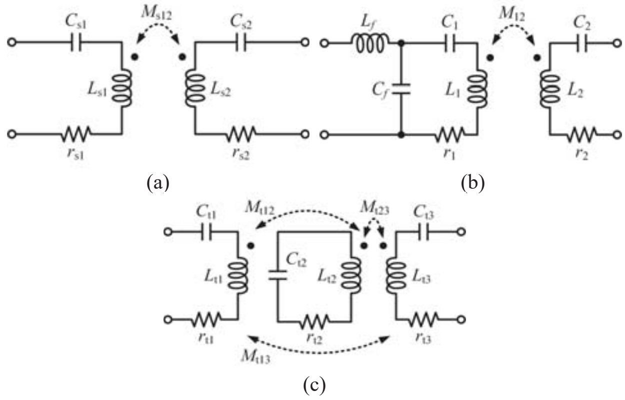

Fig. 2. Different structures of PTN. (a) SS. (b) LCC-S. (c) Three-coil.

where L_f, L_1, and L_2 are the inductances of the compensated inductor, transmitter coil, and receiver coil, respectively; C_f, C_1, and C_2 are the compensation capacitors.

For the three-coil network in Fig. 2(c), L_{t1}, L_{t2}, and L_{t3} are the self-inductances of the transmitter coil, relay coil, and receiver coil, respectively; C_{t1}, C_{t2}, and C_{t3} are the compensation capacitances of the transmitter coil, relay coil, and receiver coil respectively, r_{t1}, r_{t2}, and r_{t3} are the internal resistances of each coil, respectively; M_{t12} is the mutual inductance of the transmitter coil and relay coil, M_{t23} is the mutual inductance of the relay coil and receiver coil, M_{t13} is the mutual inductance of transmitter coil and receiver coil.

III. Analysis and Comparison of Different Networks

A. Coil Parameters

To simplify the analysis, take the SS network with symmetrical coils as an example, and its parameters are listed in Table I. Due to the limit space, the area of the coil should be carefully considered for the EVs application. To fully use this area, the shape of this example is selected to be square, which means the inductance of this shape will be a little larger than that of the circular shape [11]. And the three-coil structure is shown in Fig. 3.

For the three-coil network, the turn ratio can be defined as

$$n = N_1 / N_t \tag{6}$$

where N_1 is the number of turns of the transmitter coil L_{t1}.

Noticed that the number of turns of the relay coil should be equal to N_t - N_1 for the structure design. For a fair comparison, the transmitter (L_1) and receiver (L_2) coils of the LCC-S network are set with the same windings as the SS network.

A 3D FEA tool is used to model the networks. Fig. 4 shows the relationship between the coil parameters and the turn ratio n. An increasement of n means an increase in the width of the transmitter coil and a decrease in the width of the relay coil in the three-coil network. In the meanwhile, the self-inductance of the transmitter coil increases while the self-inductance of the relay coil decreases. Naturally, when the coupling coefficient k_{t13} increases, k_{t23} would decreases. However, k_{t12} slightly

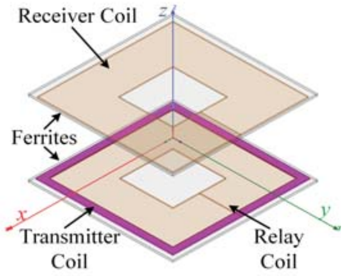

Fig. 3. The structure of three-coil.

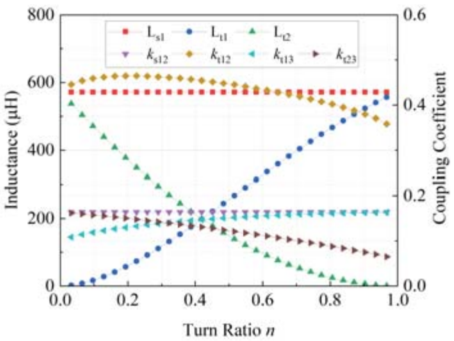

Fig. 4. Self-inductance and coupling coefficient of three-coil network with the change of n.

increases first and then decreases. The following analysis is based on the specifications defined in Table II.

B. Static Performance

When the EV is parked within the charging region, the WPT system then works automatically. Considering the receiver coil is aligned with the transmitter coil due to the assist of the auto-driving system, the static performances should be analyzed to guide the design.

In general, the conditions include adjusting the working frequency and the input voltage amplitude which corresponds to the frequency control and voltage regulation control, respectively. However, once the parameters of the network are fixed, the output power and the power transfer efficiency will not be changed with voltage regulation. Hence, this section focuses on the influence of frequency regulation.

The working frequency verse the characteristics are shown in Fig. 5. The networks are designed at 85kHz with the load:

$$R_L = 8 \cdot U_{dc}^2 \Big/ \left(\pi^2 \cdot P_o\right) \quad (7)$$

To satisfy the output power and output voltage at the aligned position and rated frequency, the RMS values of the input voltage of the SS network and the LCC-S network are 462V and 369V respectively. Besides, for the three-coil network with different n, the RMS values of input voltage are 356V, 1.02kV and 1.72kV corresponding to the case of n = 0.161, n = 0.484 and n = 0.806 respectively. It is noted that the higher n is, the higher voltage is to meet the requirements.

TABLE I. PARAMETERS OF THE SYMMETRICAL SS NETWORK

Parameters	Symbol	Value
Outer length	-	380mm
Inner length	-	150mm
Wire diameter	-	2.71mm
Number of turns of the transmitter coil	N_t	31
Number of turns of the receiver coil	N_r	31
Self-inductance of the transmitter coil	L_{s1}	571.72μH
Self-inductance of the receiver coil	L_{s2}	571.74μH
Coupling coefficient	k_{s12}	0.164

TABLE II. SPECIFICATION OF THE WPT SYSTEM

Parameters	Symbol	Value
Rated output power	P_o	3.3kW
Rated output voltage	U_{dc}	400V
Operating frequency	f	85kHz
Airgap	-	20cm

In Fig. 5, the SS network has two obvious bifurcation frequencies which may be harmful while the other networks show only one peak around the rated frequency. Especially for the three-coil network, no matter what value n is, it does not show the frequency splitting effect. Moreover, the voltage gain drops with the increase of n. When N_1 = 5, compared with the LCC-S network, the efficiency of the three-coil network is higher. However, the three-coil network with the all-resonant compensation method shows the capacitive impedance while the other networks achieve the zero-phase angle (ZPA) at the rated frequency, which may increase the volt-Ampere (VA) rating.

To overcome the shortage of a higher VA rating, it is necessary to discuss compensation elements' influence on the characteristics of the WPT system. Firstly, the analysis results of only adjusting the capacitance of the transmitter coil are shown in Fig. 6 with the same settings as Fig. 5, and the resistance of different capacitors is considered. For the SS network, the increasing compensation capacitance makes both the output power and voltage gain increase first and then decrease but the efficiency is almost stable. For the LCC-S network, the increasing compensation capacitance makes the efficiency increase first and then decrease but both the output power and voltage gain are stable. However, for the three-coil network, although the output power and voltage gain are slightly increased under larger capacitance, the efficiency is not sensitive to the change of the compensation capacitance.

Then, the analysis results of only adjusting the capacitance of the receiver coil are shown in Fig. 7 with the same settings as above. For the SS network, the increasing compensation capacitance makes the efficiency increase first and then decrease but the output power and voltage gain are stable. For the LCC-S network, the increasing compensation capacitance makes all the characteristics increase first and then decrease.

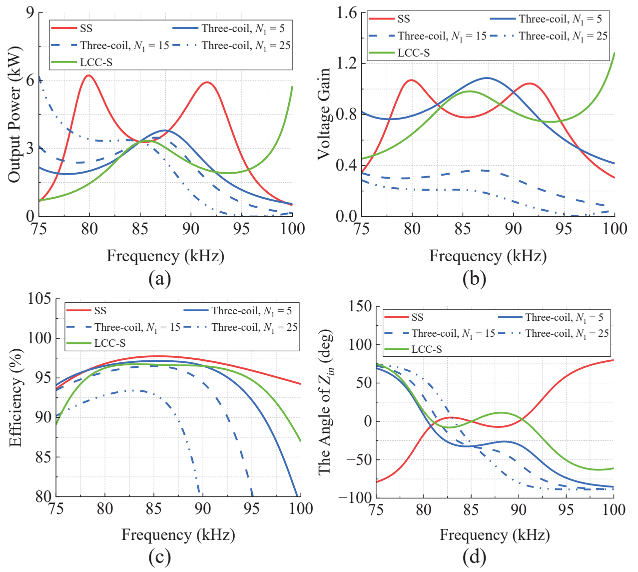

Fig. 5. Frequency vs. system characteristics. (a) Output power. (b) Voltage gain. (c) Efficiency. (d) The angle of Z_{in}.

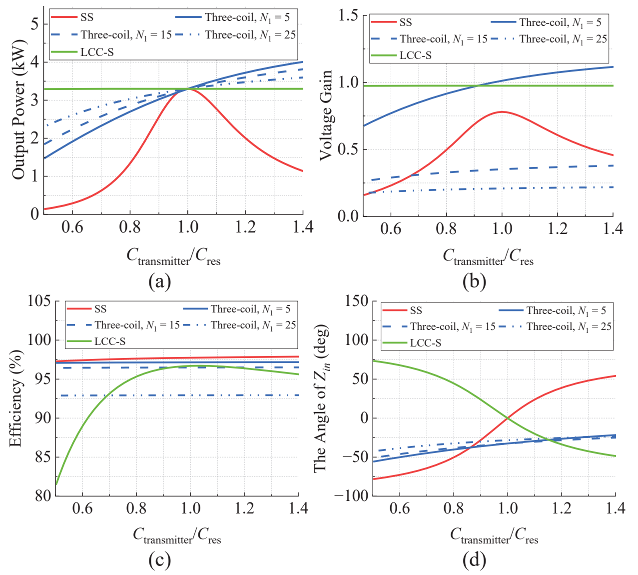

Fig. 6. Compensation capacitance of transmitter coil vs. system characteristics. (a) Output power. (b) Voltage gain. (c) Efficiency. (d) The angle of Z_{in}.

And the three-coil network performs almost like the LCC-S network.

C. Dynamic Performance

Recently, dynamic charging is getting more and more attention. In fact, lots of the transmitter coils are tiled to provide power at certain distances. However, using an inappropriate network can cause power and output voltage instability issues in the coil-to-coil transition. Fig. 8 reveals the relationship between the misalignment of the transmitter coil and receiver coil and voltage gain of the WPT system with different networks when the receiver coil moves. The voltage gain is normalized according to the value of the aligned position.

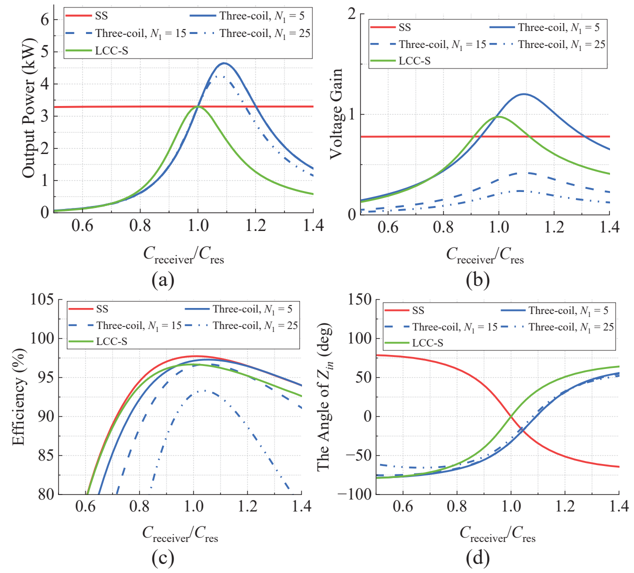

Fig. 7. Compensation capacitance of transmitter coil vs. system characteristics. (a) Output power. (b) Voltage gain. (c) Efficiency. (d) The angle of Z_{in}.

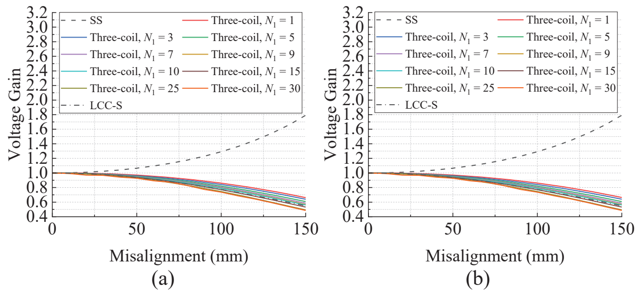

Fig. 8. Voltage gain vs. misalignment with different networks. (a) 0mm. (b) 100mm.

Besides, the values of compensation elements are fixed during the movement and designed to be full-resonance in the optimal positions where are aligned in the LCC-S network and maximum offset position (100mm) in the SS networks.

The trends of the voltage gain in the three-coil WPT system with different turn ratios are similar to that in the LCC-S WPT system, which means the outputs will be naturally reduced when the EV is driving away from the charging region while protections should be adopted in the SS WPT system. Moreover, the outputs will be more stable with a smaller n. Due to the similar voltage characteristics and the compact structure, the three-coil network has the chance to replace the LCC-S network.

IV. Design of Three-coil WPT System

As analyzed above, the three-coil WPT system can be designed based on the SS WPT system. Assuming there is an SS WPT system, this section will discuss how to design the turn ratio and the compensation of the capacitances for better performance.

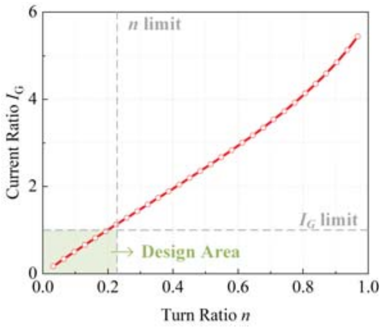

Fig. 9. Turn ratio n vs. current ratio I_G.

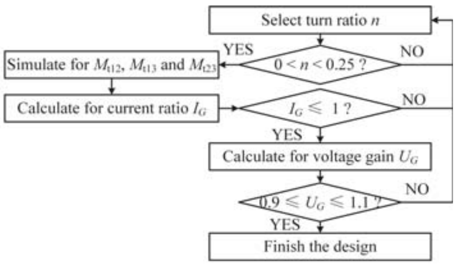

Fig. 10. The design process of the turn ratio n.

A. Turn Ratio

Fig. 10 illustrates the design process of the turn ratio. The existence of the mutual inductance between the transmitter coil and the receiver coil in the three-coil WPT system may bring some problems, such as the shift of the maximum efficiency [1] and the bifurcation phenomenon. Hence, the turn ratio should be as lower as possible. Since the inherent resistances of the coils influence the efficiency and slightly the voltage, the ideal circuit model will be used in this section. According to Fig. 2(c), the voltage gain can be expressed as

$$U_G = \left|\frac{U_o}{U_i}\right| = \left|\left(M_{t23} + M_{t13}\cdot\frac{I_i}{I_r}\right)\middle/\left(M_{t12} - M_{t13}\cdot\frac{I_o}{I_r}\right)\right| \quad (8)$$

Besides, the current ratio can be expressed as

$$I_G = \left|I_o/I_i\right| = M_{t12}/M_{t23} \quad (9)$$

According to equation (9), the relationship between n and I_G is shown in Fig. 9. Basically, I_G should not exceed 1 and better close to 1, which means the transmitter coil can use the same radius of the wires as the receiver coil. Because of that, n could be further limited to be lower than 0.25 in this case.

Moreover, the voltage gain usually is designed to 1, but in the practice, the voltage gain will shift a little (no more than 10%). Hence, to obtain the rated output power and the rated voltage, n should satisfy three conditions:

- $0 < n < 0.25$,
- $I_G \leq 1$,
- $0.9 \leq U_G \leq 1.1$.

B. Compensation of the Capacitances

The three-coil WPT system with the all-resonant compensation method shows relatively better performances than the other two WPT systems. However, higher efficiency and ZPA can be realized by redesigning the compensation of the capacitances.

The maximum efficiency can be achieved with the slightly higher compensation receiver capacitance and the lower compensation relay capacitance. Since the efficiency under the resonant compensation capacitance of the receiver coil condition is so close to the maximum, the compensation of the capacitance C_{t3} can be given by

$$C_{t3} = 1/\omega^2 L_{t3} \quad (10)$$

Then, the compensation of the capacitance C_{t2} can be adjusted to further improve the efficiency which can be described as

$$\eta = cR_L/\left(ar_{t1} + br_{t2} + cr_{t3}\right) \quad (11)$$

where

$$a = \left(\omega^2 M_{t13} M_{t23}\right)^2 + \left[\omega M_{t12}\left(r_{t3} + R_L\right)\right]^2,$$
$$b = \left(\omega^2 M_{t12} M_{t23} - \omega M_{t13} X_{t2}\right)^2 + \left(\omega M_{t13} r_{t2}\right)^2,$$
$$c = \left[r_{t2}\left(r_{t3} + R_L\right) + \omega^2 M_{t23}^2\right]^2 + \left[X_{t2}\left(r_{t3} + R_L\right)\right]^2,$$
$$X_{t2} = \omega L_{t2} - 1/\left(\omega C_{t2}\right).$$

The optimal X_{t2} can be calculated by

$$\frac{\partial \eta}{\partial X_{t2}} = 0 \quad (12)$$

Then, C_{t2} can be calculated by

$$C_{t2} = 1/\left(\omega^2 L_{t2} - \omega X_{t2}\right) \quad (13)$$

The minimum VA rating and ZPA conditions can be achieved by adjusting the compensation capacitance of the transmitter coil, which means the imaginary part of the input impedance is zero.

V. Simulation and Experimental Results

According to the designs in Section IV, the number of turns of the transmitter coil is 5. And the experimental setup is shown in Fig. 11. A Chroma 62150H-1000 is used as the DC power source. A full-bridge inverter circuit is designed with four N-channel power MOSFETs of C3M0065100K, and four diodes of RURG80100 are used in the full-bridge rectifier circuit. An ITECH IT8912E-600-840 is utilized as the DC load. Additionally, the capacitors are designed at 85kHz. To get more exact results, the values and waveforms of the DC-DC efficiency, voltage, and power are directly measured by the power analyzer of ZLG PA8000 and oscilloscope of ZLG ZDS4024.

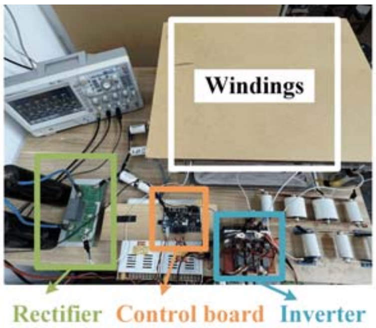

Fig. 11. Experimental setup.

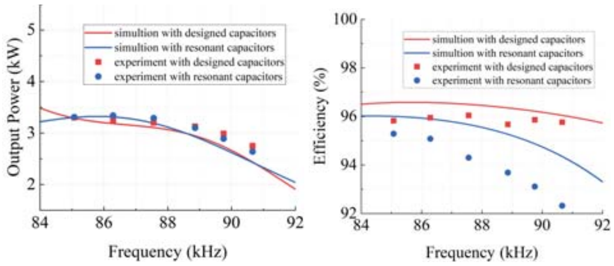

(a) (b)

Fig. 12. Frequency vs. system characteristics. (a) Output power. (b) Efficiency.

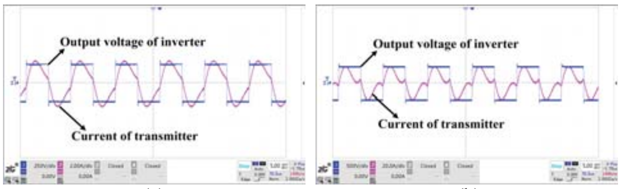

(a) (b)

Fig. 13. Waveforms of the system. (a) WPT system with designed capacitors. (b) WPT system with resonant capacitors.

A comparison of the output power and the efficiency is shown in Fig. 12. In this experiment, the DC input voltage is maintained at the value which can output 3.3kW at 85kHz exactly. The DC input voltage of the system with designed capacitors is 247V while it is 445V in the system with resonant capacitors. The lower DC input voltage to reach the rated output power is needed in the proposed system.

Besides, the trends of both experimental output power and AC-AC efficiency are well-matched with the simulation results. However, the gap difference between the simulated and experimental efficiency is because the simulation efficiencies are calculated without the losses of both inverter and rectifier. Apparently, the AC-AC efficiency can maintain at around 96.67% even if the frequency is changing, which is better than the resonance one. The voltage and current waveforms are measured to further prove the benefits of the proposed system as shown in Fig. 13.

VI. Conclusion

In this paper, different PTNs of the WPT system are theoretically analyzed and compared based on circuit theory and simulations. The effects of frequency and load are simulated to evaluate the benefits of the three-coil structure. Besides, the dynamic characteristics are also analyzed to further prove that the characteristics of the three-coil WPT system are quite similar to the other two WPT systems including SS and LCC-S structures. Due to this, the three-coil WPT system could replace others while used for EV charging with the proposed designs of the turn ratio and compensated capacitors. Finally, we obtain experimental results with 3.3kW output and 96.67% total efficiency, using a split transmitting three-coil network.

References

[1] H. Wang, K. W. E. Cheng, X. Li and J. Hu, "A Special Magnetic Coupler Structure for Three-Coil Wireless Power Transfer: Analysis, Design, and Experimental Verification," IEEE Transactions on Magnetics, vol. 57, no. 11, pp. 1-8, Nov. 2021.

[2] S. Li and C.C. Mi, "Wireless Power Transfer for Electric Vehicle Applications," IEEE Journal of Emerging and Selected Topics in Power Electronics, vol. 3, no. 1, pp. 4-17, March 2015.

[3] Q. Zhu, L. Wang, Y. Guo, C. Liao and F. Li, "Applying LCC Compensation Network to Dynamic Wireless EV Charging System," IEEE Transactions on Industrial Electronics, vol. 63, no. 10, pp. 6557-6567, Oct. 2016.

[4] Y. Lin, Z. Geng, S. Jiang, and C. Wang, "Analysis and Design of an S/PS−Compensated WPT System with Constant Current and Constant Voltage Charging," Electronics, vol. 11, no. 9, pp. 1488, May 2022.

[5] J. Yang, X. Zhang, K. Zhang, X. Cui, C. Jiao and X. Yang, "Design of LCC-S Compensation Topology and Optimization of Misalignment Tolerance for Inductive Power Transfer," IEEE Access, vol. 8, pp. 191309-191318, 2020.

[6] W. Li, H. Zhao, J. Deng, S. Li and C. C. Mi, "Comparison Study on SS and Double-Sided LCC Compensation Topologies for EV/PHEV Wireless Chargers," IEEE Transactions on Vehicular Technology, vol. 65, no. 6, pp. 4429-4439, June 2016.

[7] W. X. Zhong, C. Zhang, X. Liu and S. Y. R. Hui, "A Methodology for Making a Three-Coil Wireless Power Transfer System More Energy Efficient Than a Two-Coil Counterpart for Extended Transfer Distance," IEEE Transactions on Power Electronics, vol. 30, no. 2, pp. 933-942, Feb. 2015.

[8] J. Zhang, X. Yuan, C. Wang and Y. He, "Comparative Analysis of Two-Coil and Three-Coil Structures for Wireless Power Transfer," IEEE Transactions on Power Electronics, vol. 32, no. 1, pp. 341-352, Jan. 2017.

[9] L. Yang, X. Li, S. Liu, Z. Xu, C. Cai and P. Guo, "Analysis and Design of Three-Coil Structure WPT System With Constant Output Current and Voltage for Battery Charging Applications," IEEE Access, vol. 7, pp. 87334-87344, 2019.

[10] D. W. Seo, "Design Method of Three-Coil WPT System Based on Critical Coupling Conditions," IEEE Journal of Emerging and Selected Topics in Power Electronics, vol. 9, no. 3, pp. 3802-3811, June 2021.

[11] T. Bouanou, H. E. Fadil, A. Lassioui, O. Assaddiki and S. Njili, "Analysis of Coil Parameters and Comparison of Circular, Rectangular, and Hexagonal Coils Used in WPT System for Electric Vehicle Charging," World Electric Vehicle Journal, vol. 12, no. 1, pp. 45, Mar. 2021.